© 2016. Published by The Company of Biologists Ltd | Journal of Cell Science (2016) 129, 2030-2042 doi:10.1242/jcs.180315

RESEARCH ARTICLE

Vimentin filaments regulate integrin–ligand interactions by binding to the cytoplasmic tail of integrin β3

Jiyoon Kim[1,*], Chansik Yang[1,2,*], Eun Jin Kim[1], Jungim Jang[3], Se-Jong Kim[1], So Min Kang[1], Moon Gyo Kim[4], Hosung Jung[3], Dongeun Park[2] and Chungho Kim[1,‡]

ABSTRACT

Vimentin, an intermediate filament protein induced during epithelial-to-mesenchymal transition, is known to regulate cell migration and invasion. However, it is still unclear how vimentin controls such behaviors. In this study, we aimed to find a new integrin regulator by investigating the H-Ras-mediated integrin suppression mechanism. Through a proteomic screen using the integrin β3 cytoplasmic tail protein, we found that vimentin might work as an effector of H-Ras signaling. H-Ras converted filamentous vimentin into aggregates near the nucleus, where no integrin binding can occur. In addition, an increase in the amount of vimentin filaments accessible to the integrin β3 tail enhanced talin-induced integrin binding to its ligands by inducing integrin clustering. In contrast, the vimentin head domain, which was found to bind directly to the integrin β3 tail and compete with endogenous vimentin filaments for integrin binding, induced nuclear accumulation of vimentin filaments and reduced the amount of integrin–ligand binding. Finally, we found that expression of the vimentin head domain can reduce cell migration and metastasis. From these data, we suggest that filamentous vimentin underneath the plasma membrane is involved in increasing integrin adhesiveness, and thus regulation of the vimentin–integrin interaction might control cell adhesion.

KEY WORDS: Integrin, Vimentin, Integrin activation, H-Ras, Talin

INTRODUCTION

Precise regulations of cell–matrix interactions and cell adhesion play pivotal roles in many biological processes, such as cell growth, differentiation, formation of blood vessels, axon guidance, wound healing, immune responses, hemostasis and other important functions (Gumbiner, 1996; Hynes, 2002). Integrins, heterodimeric transmembrane proteins composed of α and β subunits, are major cell adhesion receptors that control cell adhesion (Hynes, 2002). Owing to the importance of integrins in these diverse biological functions and their potential as a target for treatment of many different human diseases caused by improper cell adhesion (Goodman and Picard, 2012), the regulatory mechanism of integrin-mediated cell adhesion has been studied extensively (Kim et al., 2011; Shattil et al., 2010). These efforts have resulted in identification of many integrin regulators that bind to integrin cytoplasmic tails, such as talin (Calderwood et al., 1999; Tadokoro et al., 2003), filamin (Lad et al., 2008), Gα13 (Gong et al., 2010), kindlin (Harburger et al., 2009; Moser et al., 2009) and others (Kim et al., 2011; Ye et al., 2014).

Talin, one of the best studied integrin activators, consists of an N-terminal ∼50-kDa globular head and a ∼220-kDa C-terminal rod domain. The talin head domain (THD) can be divided into four subdomains, F0, F1, F2 and F3 (Elliott et al., 2010), and the F3 subdomain contains the integrin-binding site (Calderwood et al., 2002). The head domain has a sixfold higher binding affinity than full-length talin for the integrin β tail, suggesting that the integrin-binding site in talin is masked in full-length talin (Yan et al., 2001). In agreement with this, overexpression of the THD or talin F2F3 domain (talin F23) activates integrin, whereas overexpression of full-length talin has little effect on integrin activation (Han et al., 2006). Thus, the integrin-binding site in talin might be unmasked by intracellular signaling during integrin activation (Calderwood, 2004). It has been suggested that the small G protein Rap1 (which has two isoforms, Rap1a and Rap1b) is involved in this unmasking process (Han et al., 2006). Upon activation by protein kinase C, Rap1 is localized to the plasma membrane and recruits its effector molecule, Rap1-GTP-interacting adaptor molecule (RIAM, also known as APBB1IP) (Han et al., 2006; Wynne et al., 2012), which binds to talin to reveal the integrin-binding site (Chang et al., 2014; Yang et al., 2014).

Some studies have found that other small G proteins are also involved in the integrin activation process (Kinbara et al., 2003). For example, a constitutively active form of R-Ras enhances integrin activation (Zhang et al., 1996), presumably through the activation of phosphatidylinositol-3 kinase (Berrier et al., 2000) and/or the integrin-binding protein filamin (Gawecka et al., 2010). In contrast, a constitutively active form of H-Ras is known to suppress integrin activation by activating Raf and its downstream kinases ERK1 and ERK2 (ERK1/2, also known as MAPK3 and MAPK1, respectively) (Hughes et al., 1997). These Ras signaling pathways might activate an integrin regulator, other than talin, that can bind to integrins and regulate their function, and regulator binding can be a promising therapeutic target for treatment of integrin-mediated diseases. However, unlike the Rap1-mediated integrin activation signaling cascade, the detailed molecular mechanisms of how Ras signaling pathways activate integrins are still unknown. Thus, we chose to study the H-Ras signaling pathway and investigated how H-Ras is involved in integrin suppression with the aim to find a new integrin regulator.

In the effort to find such an integrin regulator, we identified vimentin in its filament form as an integrin regulator. Involvement of vimentin in integrin-mediated cell adhesion and migration has been demonstrated in many studies (Satelli and Li, 2011). During the epithelial-to-mesenchymal transition (EMT), when benign epithelial tumor cells turn into highly invasive malignant tumor cells, vimentin expression is induced and even used as a molecular

[1]Department of Life Sciences, Korea University, Seoul 136-701, Republic of Korea. [2]School of Biological Sciences, Seoul National University, Seoul 151-747, Republic of Korea. [3]Department of Anatomy, Brain Research Institute, and Brain Korea 21 PLUS Project for Medical Science, Yonsei University College of Medicine, Seoul 120-752, Republic of Korea. [4]Department of Biological Sciences, Inha University, Incheon 402-720, Republic of Korea.
*These authors contributed equally to this work

‡Author for correspondence (chungho@korea.ac.kr)

Received 10 September 2015; Accepted 31 March 2016

Journal of Cell Science

Journal of Cell Science (2016) 129, 2030-2042 doi:10.1242/jcs.180315

marker for EMT (Thiery, 2002). In addition, vimentin-deficient mice have severe defects in the wound healing process (Eckes et al., 2000). The cellular localization of vimentin filaments, which are connected to focal adhesions, presumably through vimentin–plectin–integrin-β3 interaction, also indicates a possible role of vimentin in integrin regulation (Bhattacharya et al., 2009; Eckes et al., 1998; Tsuruta and Jones, 2003). Moreover, knocking down the expression of vimentin significantly reduces cell adhesiveness under conditions of flow (Bhattacharya et al., 2009). Despite these reports suggesting a role of vimentin in integrin function, the exact molecular mechanism as to how vimentin regulates cell adhesion and migration has remained unclear. In this study, we suggest that vimentin filaments underneath the plasma membrane can provide integrin attachment sites by direct interaction with integrin tails. These interactions can result in integrin clustering and enhanced integrin-mediated cell adhesion. Thus, our study helps explain how vimentin can control integrin-mediated cellular processes, such as adhesion, migration and invasion. We also suggest that disrupting the integrin–vimentin interaction could be a promising therapeutic strategy to inhibit human diseases caused by unwanted adhesion.

RESULTS

H-Ras signaling suppresses integrin activation through a talin-independent mechanism

We first investigated the relationship between the H-Ras signaling and the well-known talin-mediated integrin activation process to gather information on the unidentified effector of H-Ras signaling. Because unmasking of the integrin-binding site in talin is known to be required for talin-induced integrin activation (Yang et al., 2014), the H-Ras signaling pathway might exert its effects by regulating a signaling pathway that promotes such an unmasking process. To test this idea, we transfected talin F23 into integrin-αIIbβ3-expressing Chinese hamster ovary cells (denoted CHO/αIIbβ3), together with a constitutively active form of H-Ras, H-Ras(G12V). We stained the cells with PAC1, an antibody specific to active integrin αIIbβ3. Although talin F23 can bypass the unmasking process for integrin activation, expression of H-Ras(G12V) still inhibited the talin-F23-induced integrin activation (Fig. 1A,B) suggesting that H-Ras signaling is not be involved in the unmasking process. Next, we examined whether H-Ras signaling could directly regulate the affinity of talin for the integrin β tail, for example, through modification of talin. To this end, we used a CHO cell line stably expressing Raf fused to the estradiol receptor (denoted CHO/RafER), in which Raf–ERK signaling can be activated by 4-hydroxytamoxifen (4-OHT) to turn on integrin suppression (Hughes et al., 1997). The THD and talin F23 expressed in CHO/RafER cells were pulled down by beads bound to the integrin β1 tail protein, but the pulldown efficiency of wild-type talin was reduced compared to that of THD or talin F23 (Fig. 1C). These data support the hypothesis that the integrin-binding site is masked in wild-type talin. Importantly, activation of Raf by 4-OHT treatment did not change the interaction between the integrin β tail and talin proteins (Fig. 1C). Thus, H-Ras signaling might not regulate the affinity of talin for integrin.

As another possible suppressive mechanism, we hypothesized that H-Ras might recruit a competitive inhibitor for talin binding to integrin. If this hypothesis is correct, an excess amount of talin F23 would prevent the binding of the putative competitive inhibitor and overcome the suppression caused by H-Ras signaling. We found that increasing amounts of talin F23, co-expressed with a fixed amount of H-Ras(G12V), in CHO/αIIbβ3 cells, did not overcome this suppression (Fig. 1D). In contrast, the suppressive effect of an artificial competitive inhibitor, a talin F23(L325R) mutant that binds but does not activate integrin (Wegener et al., 2007), was overcome by overexpression of wild-type talin F23 (Fig. 1D). From these observations, we conclude that generation of a competitive inhibitor for the talin–integrin interaction might not be the way by which H-Ras suppresses integrin affinity. Instead, the inability of excess talin to overcome the H-Ras-mediated suppressive effect suggests that H-Ras can modulate the function of integrin in a way that does not change the talin–integrin interaction.

The integrin β tail is the primary site for the regulation of integrin affinity by known regulators (Kim et al., 2011; Shattil et al., 2010). To determine whether the integrin β tail is required for H-Ras signaling to suppress integrin activation, we constructed a truncation mutant that lacked the β tail (integrin αIIbβ3Δ717). Using this mutant, we tested whether the integrin β tail was involved in H-Ras-mediated suppression of integrin activation. We found that PAC1 binding to αIIbβ3Δ717 was unchanged by H-Ras(G12V), whereas PAC1 binding to wild-type integrin was increased by talin F23 and decreased by H-Ras(G12V), as expected (Fig. S1). These results suggest that the integrin β tail is required for the suppressive effect of H-Ras signaling on integrin activation.

H-Ras signaling negatively regulates the vimentin–integrin interaction, which can control integrin avidity

Results described above suggest that H-Ras might (1) recruit an integrin inhibitor that binds to the integrin β tail, or (2) induce dissociation of an integrin activator from the tail. With this information, we decided to perform a proteomic screen to identify the putative regulator, using the β3 tail protein as bait. In the screening, we tried to identify any protein that interacted with integrin differently in the absence or presence of H-Ras signaling. We found that 4-OHT treatment on CHO/RafER cells inhibited the binding of a 55-kDa protein to β3 tail (Fig. 2A), suggesting that the protein was a possible H-Ras effector. Further analysis with two-dimensional electrophoresis similarly showed that a 55-kDa spot with a pI of ∼5.0 was substantially reduced in the 4-OHT-treated condition (Fig. 2B). Using mass spectroscopy, we identified the 55-kDa protein as vimentin. Western blot analysis using an anti-vimentin antibody revealed that vimentin expressed in CHO/RafER cells was co-precipitated with beads bound to integrin β tail protein and that 4-OHT treatment reduced this binding (Fig. 2C), confirming the results from the proteomics study. The degree of vimentin binding seemed to represent different levels of vimentin in the cell extracts, because the amount of vimentin extracted from the 4-OHT-treated cells was also reduced (Fig. 2C). Indeed, the amount of detergent-soluble vimentin was substantially reduced when H-Ras(G12V) was co-transfected (Fig. 2D), presumably due to reorganization of vimentin filaments. In immunocytochemistry experiments, expression of H-Ras(G12V) resulted in the disappearance of vimentin intermediate filaments in most of the cytoplasmic areas and induced their dense localization around the nuclei (Fig. 2E, asterisks; Fig. 2F, red filled circles). In contrast, vimentin expression under standard conditions was observed to form conventional intermediate filaments all over the cytoplasm, including in the peri-membrane regions (Fig. 2E,F, red empty circles). From these results, we hypothesized that vimentin filaments localized near the plasma membrane might positively regulate integrin–ligand interactions, and one of roles of the H-Ras signaling is to induce the translocation of vimentin to the peri-nuclear region, where no vimentin–integrin interaction takes place.

With the hypothesis, we focused on the possible activating effect of vimentin filaments in integrin–ligand interactions. We observed

Journal of Cell Science (2016) 129, 2030-2042 doi:10.1242/jcs.180315

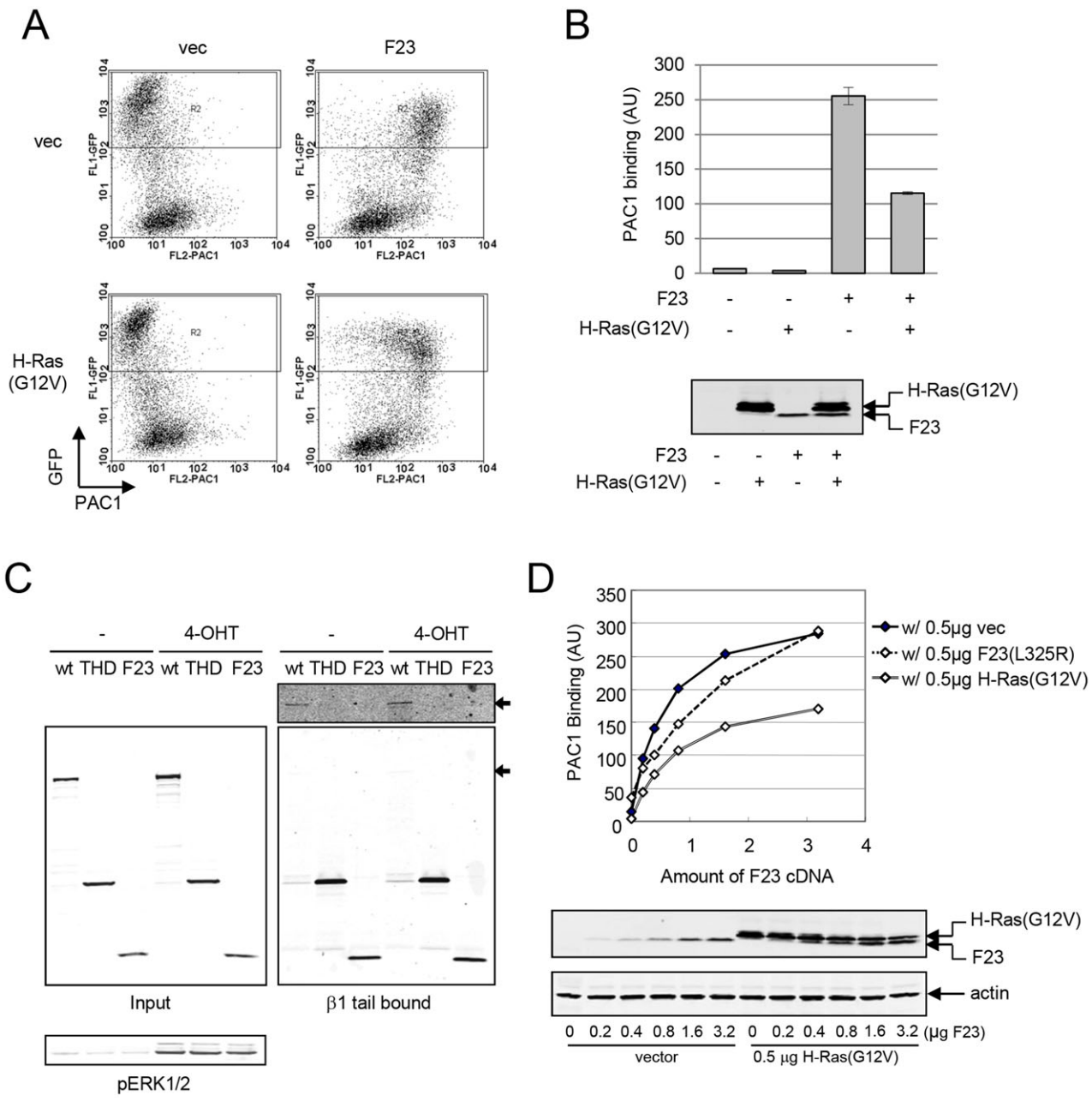

Fig. 1. The mechanism of H-Ras-induced integrin suppression. (A) CHO/αIIbβ3 cells were transfected as indicated (vec, empty vector; F23, talin F23), with GFP as a transfection marker, and binding to PAC1 was measured by flow cytometry. (B) The average mean fluorescence intensity of PAC1 in GFP-positive cells in A is shown. Error bars indicate the s.d. of triplicate samples. Protein expression was verified by western blotting. AU, arbitrary units. (C) CHO/RafER cells transfected with wild-type talin (wt), THD or talin F23 (F23) were stimulated with 300 nM 4-OHT, and the binding of these talin proteins to beads bound to integrin β1 tail was analyzed. A brightness-adjusted image is also shown for better visualization of pulled-down wild-type talin (arrows). 4-OHT-induced ERK1/2 phosphorylation was confirmed using an antibody specific for phosphorylated ERK1/2 (pERK1/2). (D) CHO/αIIbβ3 cells were transfected with increasing amounts of talin F23 and a fixed amount of empty vector (vec), H-Ras(G12V) or talin F23(L325R), together with GFP as a transfection marker. Mean fluorescence intensities of PAC1 binding in transfected cells were measured and plotted against the amount of talin F23 transfected. A representative plot from three independent experiments is shown.

that forced expression of vimentin in the presence of THD caused an increase in PAC1 binding (Fig. 3A). Therefore, we concluded that vimentin does have a role in enhancing integrin–ligand interactions. In addition, THD-induced integrin activation was significantly reduced in CHO cells stably expressing vimentin short hairpin RNA (shRNA), when compared to control-shRNA-expressing cells (Fig. 3B). We also confirmed that the surface expression level of integrin αIIbβ3 was not significantly altered by the transfection of vimentin and/or talin or by the knockdown of vimentin (Fig. 3A,B, bar graphs). In contrast to the reduced PAC1 binding observed in cells stably expressing vimentin shRNA, however, we wish to note that slight knockdown of vimentin by transient transfection of vimentin small interfering RNA (siRNA) sometimes induced an increase in PAC1 binding instead (data not shown), suggesting a complicated and context-dependent role of vimentin in integrin regulation (see Discussion). Because vimentin expression alone

Journal of Cell Science (2016) 129, 2030-2042 doi:10.1242/jcs.180315

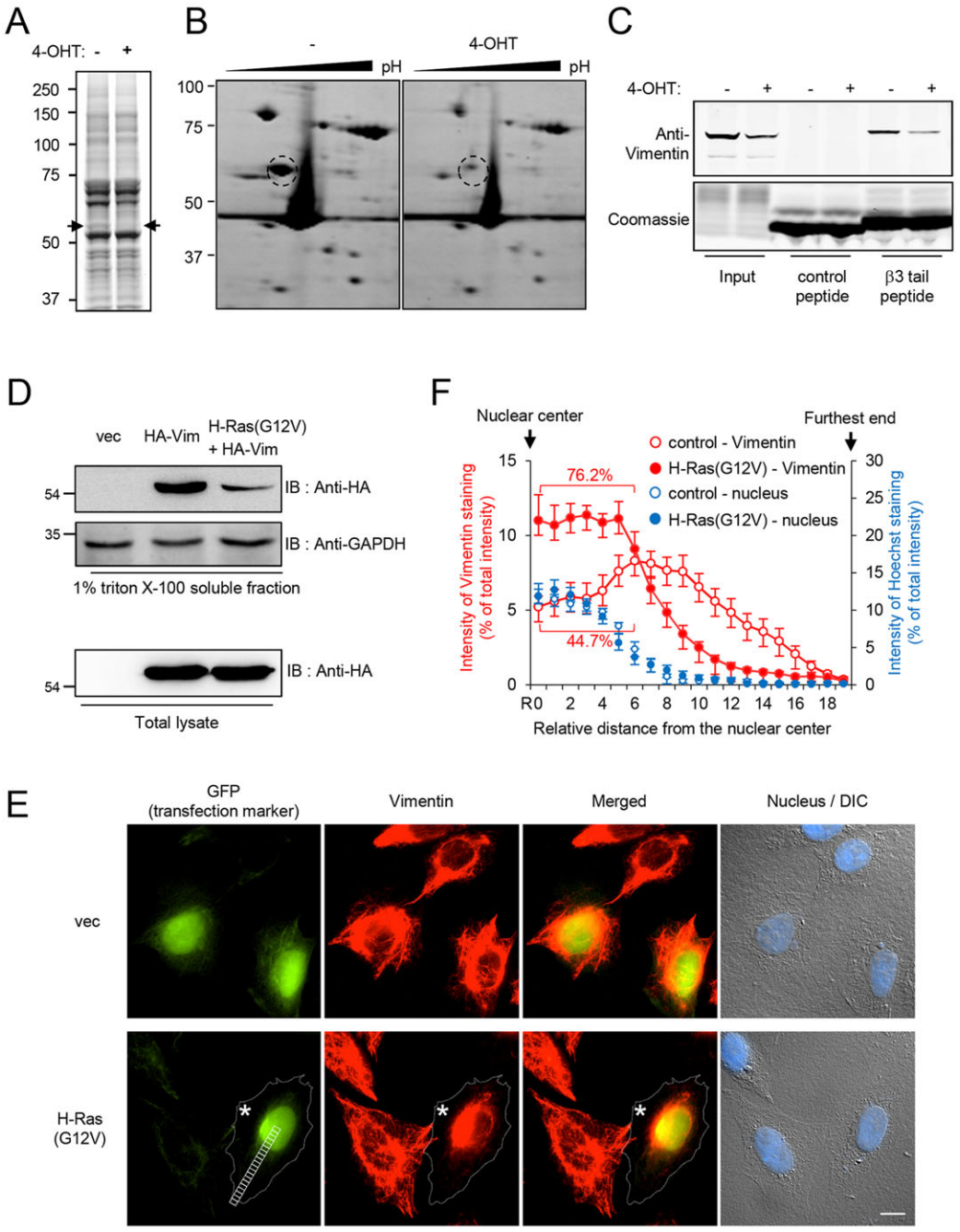

Fig. 2. Vimentin, a target of H-Ras-mediated suppression of integrin activation. (A) After CHO/RafER cells were treated with 4-OHT (or vehicle only as a control), the cell lysates were incubated with integrin β3 tail (HisAvi-β3)-bound Neutravidin beads. The bound proteins were eluted in an acidic condition and were analyzed using SDS-PAGE and subsequent Coomassie Brilliant Blue staining. A 55-kDa band (arrow) was observed in non-treated CHO/RafER cells (left lane) and is absent in 4-OHT-treated cells (right lane). (B) Proteins interacting with integrin β3 tail in CHO/RafER (treated with or without 4-OHT) were analyzed by two-dimensional gel electrophoresis and Coomassie Brilliant Blue staining. A spot with a molecular mass of 55 kDa (dotted circle) was identified as vimentin. (C) Lysates of CHO/RafER cell treated with or without 4-OHT were incubated with integrin β3 tail (or control peptide) as in (A), and the β3 tail-bound proteins were analyzed by western blotting using an anti-vimentin antibody. (D) Cells expressing HA-tagged vimentin (HA-Vim) or empty vector (vec) were transfected with or without H-Ras(G12V), and the amount of Triton-X-100-soluble vimentin was analyzed by western blotting (IB). (E) Vimentin localization (red) is shown in H-Ras(G12V)-transfected CHO/αIIbβ3 cells (asterisk) identified by co-transfected GFP expression (green). Differential interference contrast (DIC) images are also shown. Scale bar: 10 µm. (F) A rectangle was drawn from the center of nucleus to the furthest end of GFP-positive cells and the rectangle was subdivided into 20 different regions (R0–R19) as shown in E. The mean relative intensity (±s.e.m.) of vimentin staining (red) and Hoechst 33342 staining (blue) was drawn as line graphs for H-Ras(G12V)-transfected cells (closed red circles, n=14) and control cells (empty red circles, n=13). 76.2±2.6% of total vimentin staining intensity was observed in the seven regions nearest the nucleus (R0–R6) of H-Ras (G12V)-transfected cells, which is significantly higher than the 44.7±5.7% of the intensity observed in the same regions of control cells (P<0.0001, unpaired t-test).

without the THD did not increase PAC1 binding (Fig. 3A, red line), we suspected that the role of vimentin might be to induce integrin clustering leading to increased avidity for ligand binding, rather than to change the affinity state of integrin. PAC1 binding represents the combined effect of integrin affinity and integrin clustering because PAC1 is an immunoglobulin M that forms a pentamer,

Journal of Cell Science (2016) 129, 2030-2042 doi:10.1242/jcs.180315

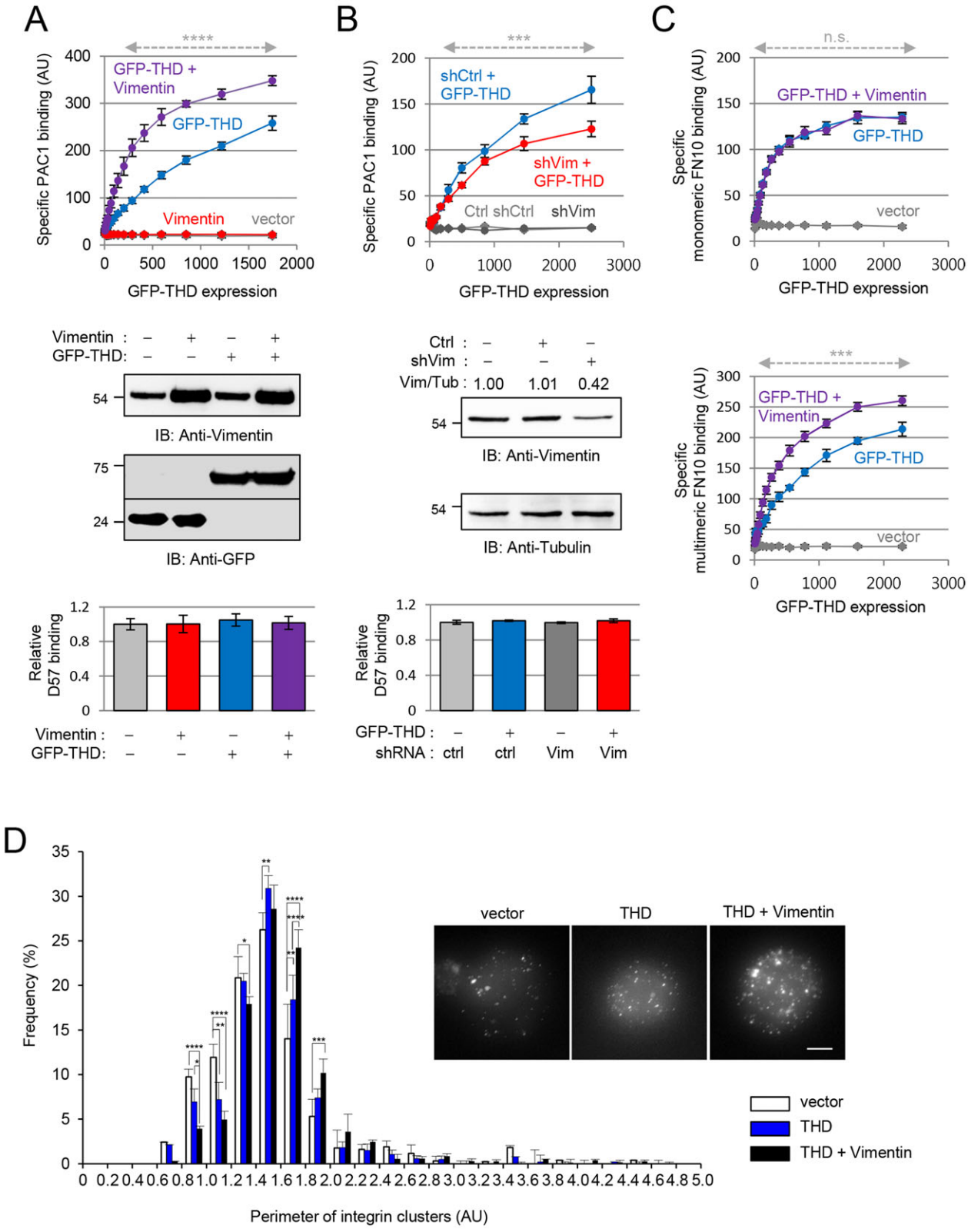

Fig. 3. See next page for legend.

providing a total of ten epitope-binding sites (Shattil et al., 1985). Thus, to specifically measure integrin affinity, we used a monomeric ligand, the tenth repeat of type III fibronectin (FN10), for which binding is dependent only on integrin affinity (Ye et al., 2013). Interestingly, we found that vimentin did not enhance THD-induced binding of FN10 (Fig. 3C, top panel). However, vimentin enhanced the binding of the multimeric ligand cross-linked FN10 (Fig. 3C, bottom panel). The fact that only the binding of a multimeric ligand, but not a monomeric ligand, to the integrin was affected by vimentin expression suggests that vimentin can increase

Journal of Cell Science (2016) 129, 2030-2042 doi:10.1242/jcs.180315

Fig. 3. Vimentin-induced increase in integrin avidity. (A) CHO/αIIbβ3 cells were transfected with GFP-tagged THD (GFP–THD) with or without vimentin. The population of stained cells was divided according to the GFP–THD expression level and the mean fluorescence intensities (MFIs) of PAC1 binding were measured. Specific PAC1 binding to cells in each region was calculated by subtraction of the MFIs in the presence of 10 mM EDTA from those in the absence of EDTA. The mean±s.e.m. of specific PAC1 binding (n=3, three independent experiments with duplicated samples) were plotted against the GFP–THD expression level (top). The specific PAC1 binding of cells co-transfected with GFP–THD and vimentin were significantly increased compared to in cells transfected with GFP–THD alone in the region indicated with the dotted gray line (****P<0.0001, Fisher's least squares difference test). Expression levels of vimentin and GFP–THD were confirmed by western blotting (IB) using anti-vimentin antibody and anti-GFP antibody, respectively (middle). Surface expression levels of integrin αIIbβ3 in cells transfected above were analyzed with complex-specific anti-integrin-αIIbβ3 antibody (D57). The bar graphs show the mean±s.e.m. (n=3) (bottom). (B) CHO cells were infected with lentivirus encoding shRNA against vimentin (shVim) or control shRNA (shCtrl). Those cells were transiently transfected with GFP–THD and specific PAC1 binding was measured as in A (top panel). In shVim-infected cells, GFP–THD-induced PAC1 binding was significantly decreased compared to in shCtrl-infected cells (***P<0.005, Fisher's least squares difference test, n=3). The expression level of vimentin (compared to tubulin, Vim/Tub) and surface expression of integrin αIIbβ3 were analyzed (middle and bottom panels). (C) CHO/αIIbβ3 cells were transfected with GFP–THD with or without vimentin, and their bindings to the monomeric ligand FN10 protein (top) and the multimeric ligand cross-linked FN10 (bottom), were measured and analyzed as in A. ***P<0.005 (Fisher's least squares difference test, n=3); n.s., not significant. (D) CHO/αIIbβ3 cells were transfected as indicated with GFP as a transfection marker. Transfected cells in suspension were stained with complex-specific anti-integrin-αIIbβ3 antibody (D57), followed by TRITC-conjugated anti-mouse-IgG antibody. Representative fluorescence images of cells are shown. Scale bar: 5 µm. The D57-positive spots in the fluorescence images were manually encircled. The perimeters of the circles were measured by NIS elements AR S/W (Nikon). The size–frequency distributions of the spots in each condition are shown in the bar graphs with error bars that represent the s.e.m. of the size frequency (n=5). A total of 366, 406 and 765 spots were analyzed in cells transfected with vector, THD and THD plus vimentin, respectively. *P<0.05, **P<0.005, ***P<0.001, ****P<0.0001 (two-way ANOVA multiple comparison using Fisher's least squares difference test).

integrin–ligand interactions by inducing the clustering of activated integrins. Consistent with this, the perimeters of the integrin αIIbβ3 clusters stained in suspended CHO/αIIbβ3 cells were significantly increased by co-expression of the THD and vimentin, when compared to cells transfected with empty vector or THD only (Fig. 3D).

The vimentin head domain binds directly to the integrin tail

Vimentin contains a non-structured head domain (denoted H) at the N-terminus, two coiled-coil domains (often denoted as C1 and C2) in the middle and a C-terminal tail domain (denoted T) (Fig. 4A) (Chernyatina et al., 2012). We examined which domain is responsible for integrin binding. We divided vimentin into N-terminal and C-terminal halves at the linker region between C1 and C2, and the binding of these constructs (expressed in CHO cells) to purified maltose binding protein (MBP)-fused integrin β3 tail was tested. We found that the vimentin head to C1 region bound to the β3 tail protein, but the C2 to tail region did not (Fig. 4B). In a subsequent experiment, we found that a purified glutathione-S-transferase (GST)-fused vimentin head domain bound directly to a purified β3 tail specifically in a concentration-dependent manner (Fig. 4C), showing that vimentin can interact directly with the integrin tail through its head domain. Deletion of 13 amino acids at the C-terminal end of β3 tail (Δ750, Fig. 4D) completely blocked the interaction, suggesting that this region is involved in the interaction. In case of the vimentin head domain, deletions after 46th amino acid (Δ46 and Δ71) did not block the interaction, but a deletion after 21st amino acid (Δ21) did (Fig. 4E). Thus, vimentin amino acids 21–45 seem to be crucial for the binding.

We thought that the observed vimentin-induced change in integrin avidity might be due to the ability of vimentin to make filamentous structures and provide many integrin-binding sites (from the vimentin head domain) under the plasma membrane. If that hypothesis is true, overexpression of a vimentin head domain that is incapable of making filamentous structures might compete with endogenous vimentin filaments for integrin binding, thus abolishing the effect on avidity. In agreement with this idea, the vimentin head domain protein inhibited the interaction between endogenous vimentin and purified β3 tail in a concentration-dependent manner (Fig. 4F). In contrast, the vimentin head domain protein did not compete with other integrin regulators, such as filamin A and talin (Fig. 4F). In addition, THD-induced β3 transmembrane domain tilting was not inhibited by the vimentin head domain in a purified system (Fig. S2), again confirming no competition between talin and vimentin. Interestingly, in agreement with the hypothesis above, expression of the vimentin head domain largely inhibited THD-induced PAC1 binding whereas surface expression of the integrin was not altered (Fig. 5A). Moreover, we observed that expression of the vimentin head domain caused detachment of vimentin filaments from the plasma membrane regions and induced vimentin aggregation near the nuclei, which is very similar to the effect of H-Ras(G12V) (Fig. 5B, asterisk). These results confirm the role of vimentin in regulating integrin–ligand interactions. Moreover, these results also suggest that integrin–ligand interactions are enhanced by the binding of vimentin filaments, not vimentin itself, to integrin.

Changes in vimentin filament organization can regulate integrin–ligand interactions

Because the integrin-binding site was mapped to the vimentin head, we assumed that the vimentin head and C1 domain protein should inhibit THD-induced integrin adhesiveness just like the vimentin head, and that the C2 and tail domain should have no effect. Very surprisingly, we found that both constructs enhanced the THD-induced PAC1 binding (Fig. 5C), although this observation was less pronounced for the head and C1 domain. Integrin surface expression was not altered by those constructs (Fig. 5C, bar graph). We examined whether the head and C1 domain, or C2 and tail domain had an intrinsic ability to increase integrin–ligand interactions. Similar to full-length vimentin, neither fragment induced PAC1 binding when expressed without THD (not shown). However, we found that these proteins destroyed the filamentous vimentin structures and induced punctuated vimentin staining patterns throughout the cells (Fig. 5D, arrows). This pattern is similar to that formed by aggregates of the vimentin filament precursor observed at the lamellipodia of migrating fibroblasts (Goldman et al., 1996; Helfand et al., 2011; Strelkov et al., 2002) or at cell adhesion sites during cell spreading (Correia et al., 1999). In agreement with our observation, short peptide either from the N- or C-terminal region of vimentin (R1 and R2 in Fig. 4A) induces fragmentation of vimentin filaments by inhibiting vimentin assembly (Goldman et al., 1996; Helfand et al., 2011; Strelkov et al., 2002). Theoretically, once vimentin filaments are converted into a large number of smaller pieces, the vimentin fragments can be released from the filamentous structure and move more freely to the plasma membrane than vimentin in the filamentous form. In

Journal of Cell Science (2016) 129, 2030-2042 doi:10.1242/jcs.180315

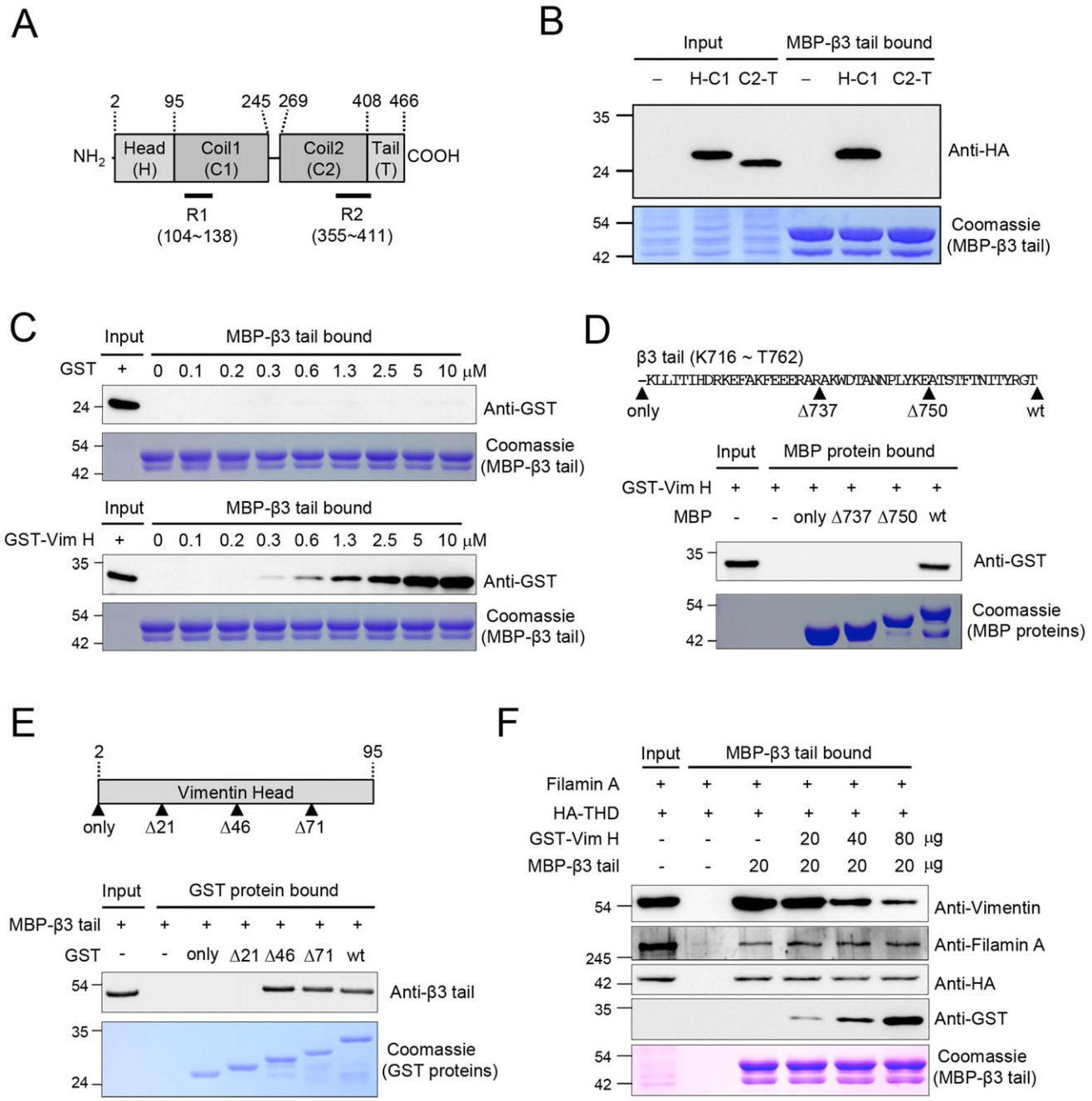

Fig. 4. Direct interaction between the vimentin head domain and the integrin cytoplasmic tail. (A) Domain structure of vimentin. R1 and R2 indicate peptide sequences that induce disassembly of vimentin filaments (Goldman et al., 1996; Helfand et al., 2011). (B) A HA-tagged vimentin head and C1 domain (H-C1) and the C2 and tail domain (C2-T) were expressed in CHO cells and tested for binding to a purified MBP-fused integrin β3 tail. (C) Binding of the purified β3 tail protein to the increasing amount of a GST-tagged vimentin head domain (Vim H) and GST is shown. (D) Interaction between the purified GST-tagged vimentin head domain and the purified MBP-tagged β3 tail protein with truncations at the positions indicated by the arrowheads was tested. (E) GST-tagged vimentin head domains with truncations at the positions indicated by the arrowheads were tested for binding to the purified β3 tail protein. (F) Lysates of CHO cells transfected with filamin A and HA–THD were incubated with beads bound to the MBP-fused β3 tail protein in the presence of increasing amounts of GST-tagged vimentin head domain. β3 tail protein bound to endogenous vimentin, filamin A, HA–THD and the vimentin head domain proteins was detected by western blotting.

addition, the filaments would contain enough vimentin molecules to mediate integrin clustering. Thus, our interpretation of these interesting phenomena is that reorganization of vimentin filaments into smaller fragments upon expression of the head and C1, or C2 and tail domain might be responsible for the enhanced integrin adhesiveness. If we consider both the positive (by inducing fragmentation of vimentin filaments) and negative (by inhibiting integrin–vimentin filament interactions) effects, the reason why the head and C1 domain induces a weaker integrin-ligand interaction than the C2 and tail domain (Fig. 5C) can also be explained.

Overexpression of vimentin head reduces cancer invasiveness

Next, we investigated the role of the vimentin–integrin interaction on cell migration and metastasis. 4T1 cells are derived from a highly invasive mouse breast cancer cell line from the BALB/c strain

Journal of Cell Science (2016) 129, 2030-2042 doi:10.1242/jcs.180315

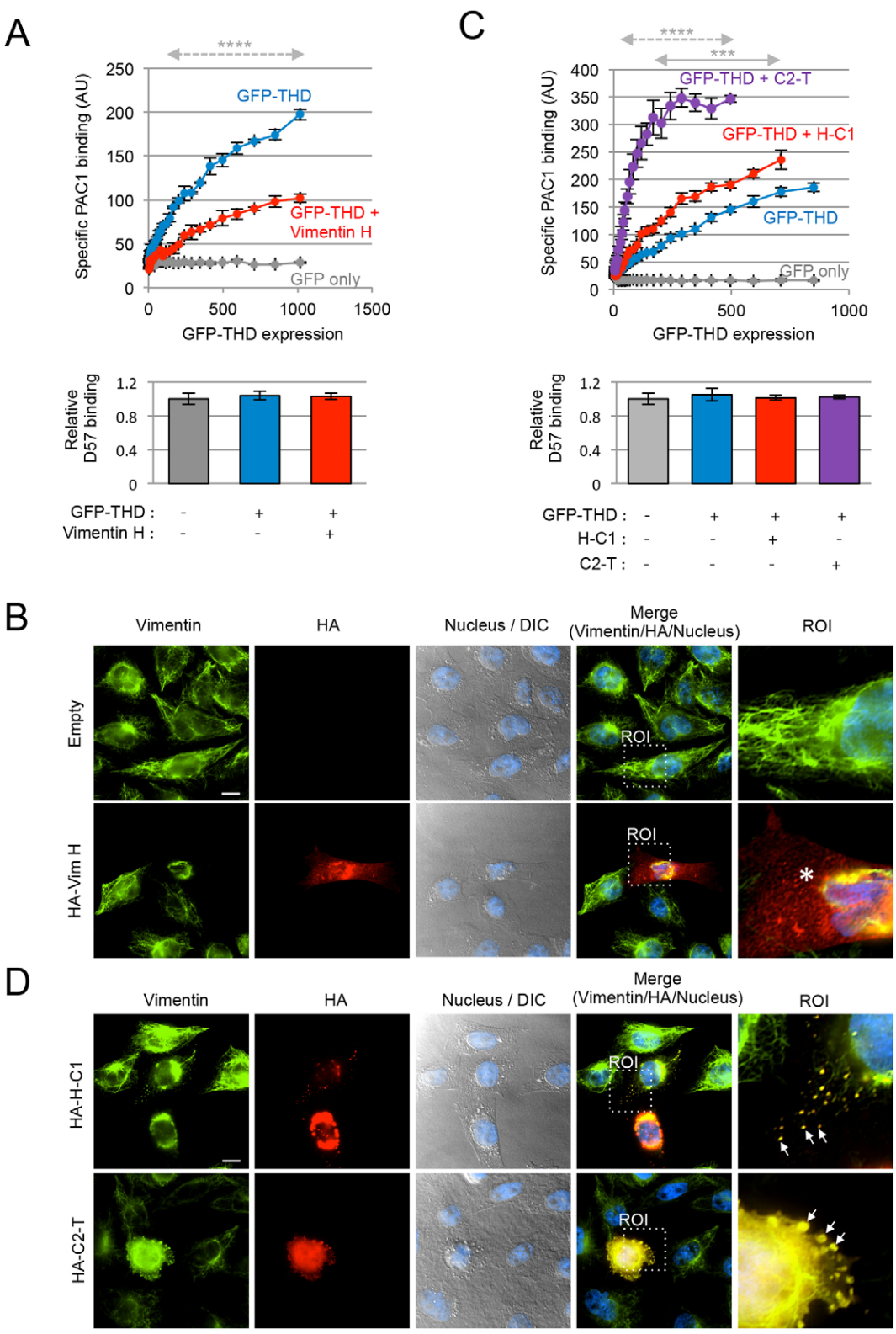

Fig. 5. See next page for legend.

(Aslakson and Miller, 1992) and expresses integrin β3 (Fig. S3A). These cells bind to fibrinogen, a ligand of β3 integrin (integrin αVβ3) expressed in non-platelet cells. This binding increased in the presence of THD and vimentin (Fig. S3B,C), similar to integrin αIIbβ3 (Fig. 3A). To see the consequence of integrin–vimentin filament interaction loss, we infected 4T1 cells with lentivirus encoding the vimentin head. The vimentin head in the lentiviral construct contains a downstream internal ribosome entry site (IRES) followed by the gene encoding GFP. Thus, we sorted GFP-positive cells and pooled them to generate a population of vimentin-head-

Journal of Cell Science (2016) 129, 2030-2042 doi:10.1242/jcs.180315

Fig. 5. Effect of vimentin filament disassembly on integrin–ligand interaction. (A) The mean±s.e.m (n=3) of specific PAC1 binding to CHO/αIIbβ3 cells expressing GFP–THD with or without the vimentin head domain (vimentin H or Vim H) are depicted as in Fig. 3A. Vimentin head domain expression significantly reduced the THD-induced PAC1 binding (****P<0.0001, Fisher's least squares difference test, n=3). The mean±s.e.m. (n=3) of D57 binding to those cells are shown as bar graphs (lower panel). (B) CHO/αIIbβ3 cells transfected with empty vector (upper panels) or HA-tagged vimentin head domain (lower panels) were stained with anti-vimentin (green) and anti-HA (red) antibodies. Nuclei were stained with Hoechst 33342 dye (blue) and merged with DIC images. Regions of interest (ROIs) indicated with dotted boxes were digitally enlarged. Note that expression of the vimentin head domain induced vimentin aggregation near the nucleus (asterisk). Scale bar: 10 µm. When analyzed as in Fig. 2F, 62.3±11.7% (mean±s.e.m.) of total vimentin staining intensity was observed in the seven regions near the nucleus (R0–R6) of cells transfected with the vimentin head domain, which is significantly higher than the 32.2±3.7% of the intensity that was observed in the same regions of control cells (P<0.05, unpaired t-test, n=5). (C) Specific PAC1 binding was analyzed in CHO/αIIbβ3 cells that were transfected with GFP–THD with or without the vimentin head and C1 domain (H-C1) and the C2 and tail domain (C2-T). The line graphs and bar graphs show the means±s.e.m. (n=3) of specific PAC1 binding and D57 binding, respectively. ****P<0.0001 (Fisher's least squares difference test, n=3, between GFP–THD+C2-T and GFP–THD samples, dotted gray arrows), ***P<0.005 (Fisher's least squares difference test, n=3, between GFP–THD+H-C1 and GFP–THD samples, solid gray arrows). (D) CHO/αIIbβ3 cells expressing HA-tagged vimentin H-C1 or vimentin C2-T were stained with anti-vimentin and anti-HA antibodies, as in B. The arrows indicate punctuated vimentin staining patterns. Scale bar: 10 µm.

expressing cells (Fig. 6A). As a control, we also collected GFP-negative cells (Fig. 6A). Although vimentin expression in both GFP-positive and -negative cells was rarely detected in normal culture conditions, treatment with transforming growth factor (TGF)-β, the signal that induces EMT (Liu et al., 2012), significantly induced vimentin expression (Fig. 6B). In our migration assay, both of these cell populations, GFP-negative and -positive cells, showed a relatively low migration rate in the absence of TGF-β (Fig. 6C). When treated with TGF-β, there was a tenfold increase in the migration rate of GFP-negative cells (Fig. 6C,D). However, in the case of GFP-positive cells, the TGF-β-induced migration was largely suppressed (Fig. 6C,D). Consistent with this result, BALB/c mice that were intravenously injected with GFP-positive 4T1 cells also exhibited a reduction in nodule formation on the lung (Fig. 6E,F). Because the effect of vimentin head must be dependent on the presence of vimentin filaments, we randomly selected metastatic nodules and examined vimentin expression in each nodule. Interestingly, induction of vimentin expression was observed in all the nodules tested [eight nodules from GFP-positive cells (Fig. 6G) and eight nodules from GFP-negative cells (data not shown)], suggesting a crucial role for vimentin in cancer metastasis. From these results, we suggest that one of the roles of vimentin during metastasis is to regulate integrin adhesiveness and that inhibition of vimentin-filament-dependent integrin regulation might reduce cell migration and metastasis. However, we do not rule out the possibility that expression of vimentin head affects other functions of vimentin involved in cell migration, rather than inhibiting the integrin-β3–vimentin-filament interaction.

DISCUSSION

In this report, we first identified vimentin filaments as new regulators for integrin function. Our study suggests that vimentin filaments underneath the plasma membrane have many vimentin heads exposed along the filaments, and thus can provide many integrin-binding sites for integrin clustering, which in turn can enhance integrin–ligand interaction (Fig. S4). Because integrins localize to the plasma membrane, this interaction is only possible near the plasma membrane. Thus, we suggest that translocation of vimentin to the peri-nuclear region, for example by H-Ras signaling, might have a negative effect on the integrin–ligand interaction. However, owing to the experimental difficulty of testing the suppressive effect of H-Ras with vimentin filaments kept intact under the plasma membrane, we were unable to determine whether the suppressive effect of the H-Ras is solely dependent on the rearrangement of vimentin filaments. Therefore, at the moment, the initial question of how H-Ras suppresses integrin function has not been fully established. Second, our study provides a possible explanation of how organization of vimentin filaments is associated with cell adhesion. Not only long vimentin filaments, but also smaller ones containing a high enough number of vimentin subunits, would induce changes in integrin clustering. Therefore, regulation of the local assembly or disassembly of vimentin filaments near the cell surface could be a way of controlling integrin-mediated adhesiveness at the region involved. Reducing vimentin expression level to a certain degree might reduce the number of the filaments near cell surface (negative effect) or induce disassembly of vimentin filaments leaving smaller filaments capable of inducing integrin clustering (positive effect). Because of these possible dual effects, we think transient knockdown of vimentin (description on Fig. 3B) might cause different results depending on the degree of knockdown efficiency and the knockdown-induced status of vimentin filaments in each experiment. Finally, our results showed that the vimentin head impairs cell migration and metastasis (Fig. 6), likely by inhibiting integrin–vimentin interaction. Unlike after the knockdown of vimentin, overexpression of the vimentin head would detach the integrin from vimentin filaments regardless of the status of the filaments, which can consistently reduce the clustering effect of vimentin. Thus, we suggest that targeting the integrin–vimentin interaction could be a potential therapeutic approach to treat cell-adhesion-mediated diseases.

It is well known that the expression of vimentin correlates with an invasive cellular phenotype, and forced expression of vimentin can convert epithelial cells into invasive mesenchymal cells (Mendez et al., 2010). Our study suggests that induction of vimentin expression during EMT can increase the overall adhesiveness of tumor cells toward the extracellular matrix (ECM). The increased cell–ECM interaction might become dominant over cell–cell interactions, which would cause individual cell migration or invasion. In addition to vimentin expression, the dynamic regulation of vimentin structure seems to be important in cell adhesion. For example, during cell adhesion, many smaller fragments of vimentin filaments are observed (Correia et al., 1999). In addition, the small fragments, which are similar to those observed in this study (Fig. 5D), have been suggested to modulate the formation of lamellipodia (Helfand et al., 2011). According to our study, vimentin filaments in mesenchymal cells might work as a reservoir for integrin regulators; once the filaments are broken into many smaller fragments in the cellular region where increased cell–ECM interaction is required, the fragments are able to modulate cell attachment at the site by increasing integrin avidity (Fig. S4). Therefore, our study can explain the role of expression and reorganization of vimentin filaments in adhesiveness.

Owing to their crucial roles in extracellular matrix binding, integrins have been considered as potential therapeutic targets to reduce unwanted cell adhesion and migration. Indeed, many anti-integrin drugs have been investigated for curing autoimmune

Journal of Cell Science (2016) 129, 2030-2042 doi:10.1242/jcs.180315

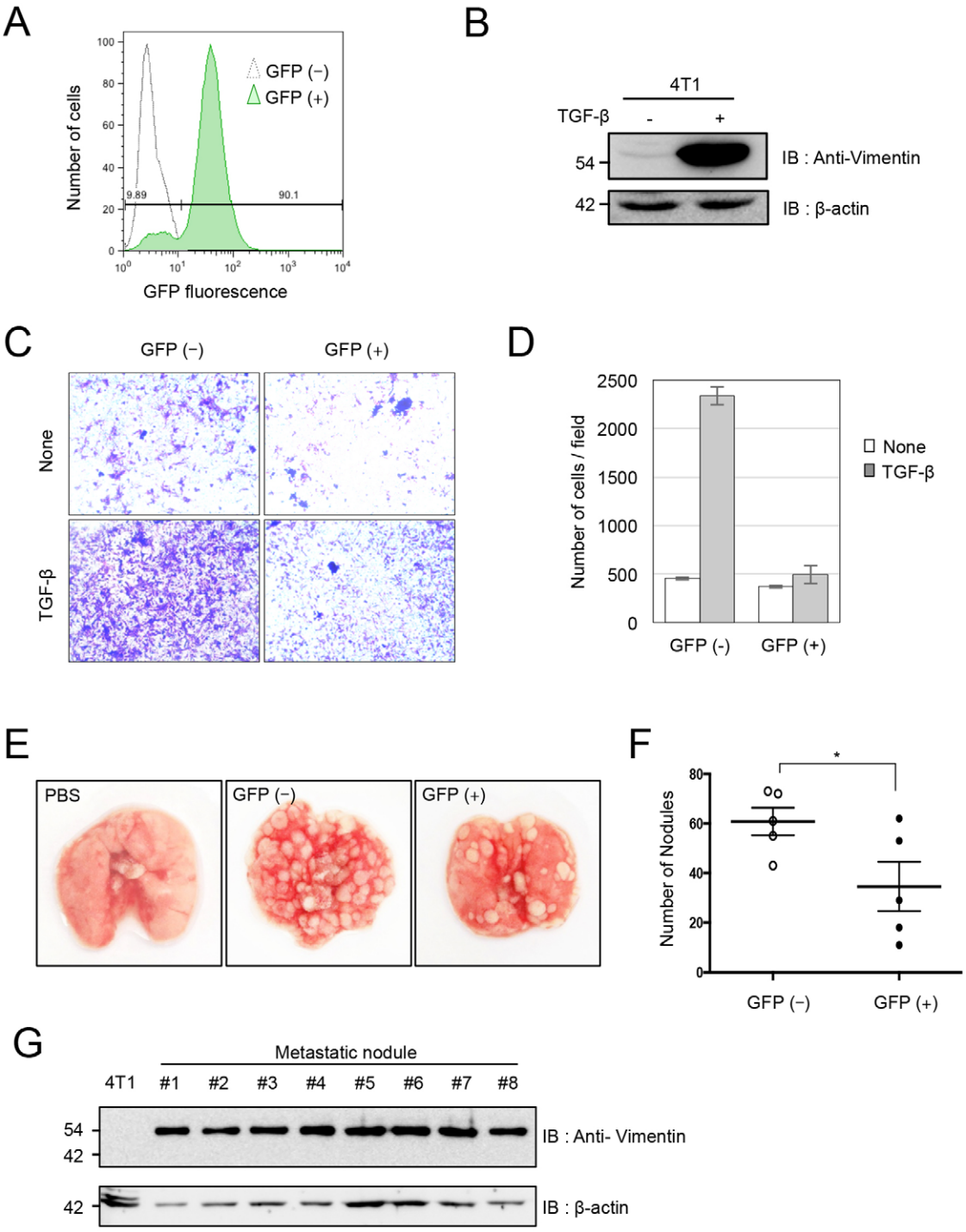

Fig. 6. Impaired cell motility upon overexpression of the vimentin head domain. (A) 4T1 cells infected with the vimentin head domain were sorted and pooled based on IRES-driven GFP expression. GFP expression profiles of GFP-negative (control) and GFP-positive (expressing the vimentin head domain) cells are shown. (B) 4T1 cells were maintained in the presence of 5 ng/ml TGF-β for 2 days and the expression of vimentin was tested by western blotting (IB). (C) GFP-positive and -negative 4T1 cells were placed in growth medium on a fibrinogen-coated upper chamber of a Transwell® culture plate in the presence or absence of 5 ng/ml TGF-β (in both the upper and lower chambers). After 20 h, cells on the opposite side of the Transwell® membrane were visualized. Representative images are shown. (D) Mean±s.e.m. numbers of migratory cells in C are shown in each condition (n=3). (E) GFP-negative or -positive cells were injected into the tail veins of BALB/c mice. After 2 weeks, mice were killed and lung metastatic nodules were visualized. (F) Numbers of lung metastasis nodules formed by GFP-negative and -positive cells were counted and plotted in the graph, with bars showing mean±s.e.m. (n=5, *P<0.05, unpaired t-test). (G) The metastatic nodules formed by GFP-negative cells were detached from the lungs and vimentin expression was visualized by western blotting (IB). Actin was used as a protein loading control.

diseases, cancer, thrombosis and so on (Goodman and Picard, 2012). However, to the best of our knowledge, there are only four integrin antagonists currently used in the clinic: three integrin αIIbβ3 antagonists, blocking platelet adhesion for the treatment of acute thrombosis, and one antagonist targeting the α4 integrin, blocking leukocyte adhesion for the treatment of autoimmune diseases. The

Journal of Cell Science (2016) 129, 2030-2042 doi:10.1242/jcs.180315

mechanism of action of these and other integrin-targeting drugs under investigation in clinical trials is direct blockage of integrin–ligand interaction by targeting the ligand-binding sites in integrins through small molecules or monoclonal antibodies (Goodman and Picard, 2012). Given the importance of integrins in normal physiology, complete blockage of integrin function might disrupt not only the newly formed cell adhesion but also the pre-existing cell adhesion, thus causing severe adverse effects such as the detachment of adherent cells, which might account for the failure of anti-integrin drugs targeting those cells. Even in floating cells, bleeding problems can occur with the use of αIIbβ3 antagonists (Quinn et al., 2003) and viral diseases can occur with the use of the α4 integrin antagonist (Langer-Gould et al., 2005). In addition, several reports have demonstrated that drugs targeting integrin–ligand binding sites can stimulate integrin signaling when in low concentration, rather than block it (Reynolds et al., 2009), presumably because the antagonizing drugs act as a ligand (agonism). Because of the mechanism-based toxicity and agonism, many attempts have been made to identify and target integrin regulators instead. These regulators might serve as an alternative way to control the function of integrins indirectly, whereby the mode of action would only target newly formed adhesions and should not have the associated adverse effects. In this regard, we propose that the integrin–vimentin interaction could be a potent target to overcome the current huddle in anti-integrin therapy. Based on our study, the inhibition of integrin–vimentin interaction significantly reduced the migration as well as metastasis of cancer cells (Fig. 6). Considering that the role of vimentin we found in our study is to induce integrin clustering and thus to enhance integrin–ligand interaction, blocking the interaction would not perturb pre-existing cell adhesion but will inhibit only new adhesion formation. At the same time, the mechanism of action will not provoke integrin signaling. Therefore, we believe that our study not only explains the role of vimentin in cell adhesion, but also provides a novel therapeutic target for treatment of cell-adhesion-mediated diseases, such as metastasis.

MATERIALS AND METHODS

Cell lines, plasmids and antibodies

CHO cells and 4T1 cells were purchased from the Korean Collection for Type Culture and the American Type Culture Collection, respectively. CHO/RafER and CHO/αIIbβ3 cells were kind gifts from Mark Ginsberg (University of California San Diego, CA), and they were authenticated by 4-hydroxytamoxifen (4-OHT) responsiveness and D57 binding, respectively, during their use. HA-tagged talin constructs (wild type, head domain and F2F3 domain), HA-tagged H-Ras(G12V), integrin αIIb and integrin β3 constructs (provided by Mark Ginsberg) were described previously (Han et al., 2006). An untagged version of H-Ras(G12V) was kindly provided by Young Do Yoo (Korea University, Seoul, Republic of Korea). The GFP-tagged THD was generated by inserting a PCR-amplified THD into pEGFP-C1 (Clontech). Vimentin cDNA was purchased from the Korea Human Gene Bank and used in PCR to generate a HA-tagged vimentin head domain (amino acid residues 2–95), a head and C1 domain (H-C1, amino acid residues 2–254), and a C2 and tail domain (C2-T, amino acid residues 255–466) construct in pcDNA3, as well as a GST-fused vimentin head domain in pGEX4T-1 (GE Healthcare). To generate the His-pMAL/β3 tail construct for purification of the maltose binding protein (MBP)–β3-tail fusion protein, the integrin β3 tail region was amplified by PCR and cloned into BamHI and XhoI sites of His-pMAL vector (provided by Hyun Kyu Song, Korea University, Seoul, Republic of Korea). Short hairpin RNA (shRNA) against vimentin was generated by ligation of annealed oligonucleotide containing the target sequence (5′-AATACCAAGACCTGCTCAATC-3′) into a lentivirus vector, pLKO.1 (Addgene). Its scrambled sequence (5′-GCAATGCATGCCATACTAACA-3′) was used to generate the control shRNA construct. These lentivirus vectors were transfected into Lenti-X 293T cell line (Clonetech) to generate lentivirus particles as previously described (Kim et al., 2012). Complex-specific anti-integrin-αIIbβ3 antibody (D57, 10 μg/ml for flow cytometry), activation-specific anti-αIIbβ3 antibody (PAC1, mouse ascetic fluid, 1:400 for flow cytometry) and anti-integrin-β3-tail antiserum (Rb8275, rabbit serum, 1:1000 for western blotting) were provided by Mark Ginsberg. Anti-vimentin (Sigma-Aldrich, V6389, 1:1000 for western blotting, 1:100 for cytochemistry), anti-HA (Santa Cruz Biotechnology, sc-805, 1:1000 for western blot, 1:100 for cytochemistry), anti-β-actin (Santa Cruz Biotechnology, sc-130656, 1:1000 dilution for western blotting), anti-GAPDH (Santa Cruz Biotechnology, sc-20357, 1:500 for western blotting), anti-GFP (Santa Cruz Biotechnology, sc-9996, 1:200 for western blotting) and anti-GST (GE Healthcare, RPN1236, 1:1000 for western blotting) antibodies were obtained commercially.

Protein purification

To prepare monovalent ligand for integrin αIIbβ3, the tenth repeat of fibronectin type III (FN10) was used as previously described (Ye et al., 2013). Briefly, pGEX-6P-1 vector containing FN10 was introduced into *E. coli* strain BL21-DE3, and protein was expressed by adding IPTG to the culture. Expressed GST–FN10 was purified using glutathione–Sepharose-4B (GS4B, GE Healthcare) according to the manufacturer's instructions. The elution buffer was exchanged to PreScission protease cleavage buffer (50 mM Tris-HCl, 150 mM NaCl, 1 mM EDTA, 1 mM DTT, pH 7.5) using Zebra™ spin desalting columns (Thermo Scientific), and the purified proteins were incubated with PreScission protease (GE Healthcare) at 4°C overnight to remove GST. The free GST was removed by incubating the mixture with GS4B for 6 h at 4°C. The flow-through was loaded to the desalting column equilibrated with PBS for the biotinlyation reaction using EZ-Link NHS-Biotin (Thermo Scientific). To prepare the multimeric ligand, purified GST–FN10 was first biotinylated and then incubated with a fourfold molar excess of 1,11-bis(maleimido)triethylene glycol [(BM(PEG)3, Thermo Scientific] at room temperature for 1 h to allow cross-linking events to occur. The reaction was treated with 20 mM DTT and incubated for 15 min at room temperature to quench all unreacted reagent, followed by a desalting step. MBP–β3-tail protein was purified from BL21-DE3 cells transformed with His-pMAL/β3 tail using amylose resin (New England BioLabs) according to the manufacturer's guide. Similarly, GST-tagged vimentin head protein was purified from BL21-DE3 cells transformed with pGEX4T-1/Vim-H using GS4B.

Pulldown assay

CHO cells transfected with various vimentin constructs were lysed with a lysis buffer [1% Triton X-100, 150 mM NaCl, 50 mM HEPES, pH 7.4, protease inhibitor cocktail (Roche)]. Cell lysates were incubated for 20 min at 4°C with agitation, homogenized by passing through a 26-gauge needle three times and then clarified by centrifugation at 17,000 ***g*** for 20 min. The cell lysates (or GST proteins as indicated) were added to purified MBP-fused integrin β3 tail (or GST-tagged vimentin head protein) and incubated for 2–16 h at 4°C with agitation. The mixtures were further incubated with amylose resin (or GS4B) for 2 h. Beads were washed three times and the bound proteins were eluted by boiling the beads in SDS-PAGE sample buffer. Eluted proteins were analyzed by western blotting using anti-vimentin antibody or anti-HA antibody.

Flow cytometry

Cells were transfected with GFP–THD (or pEGFP-C1 empty vector) and vimentin cDNAs (or empty vector) at a 1:8 ratio, as indicated in each experiment. At 24 h post transfection, cells were detached and ∼5×10^5 cells were incubated with 4 μg/ml PAC1 or 100 μg/ml biotinylated monomeric or oligomeric FN10. Specific binding was calculated as the MFI–MFI_0 [where MFI is mean fluorescence intensity of binding of each ligand and MFI_0 is mean fluorescence intensity of the binding in the presence of 10 mM EDTA (for PAC1 binding) or 100 μM integrilin, an integrin-αIIbβ3-specific inhibitor (for monomeric or cross-linked FN10 binding)]. Because monomeric and cross-linked FN10 might bind to endogenous integrins in CHO/αIIbβ3 cells, only the integrin-inhibitable binding was considered as specific FN10 binding to integrin αIIbβ3 (Ye et al., 2013). The reaction was incubated for 30 min at room temperature. For monomeric or cross-linked

FN10-binding assays, cells were fixed with 3.7% formaldehyde for 10 min after the incubation. After washing, cells were further incubated with fluorophore-conjugated secondary reagents, allophycocyanin-conjugated anti-IgM or streptavidin. The stained cells were analyzed using a FACSCalibur (BD Biosciences). Dot plots were generated by WinMDI (Scripps institute). MATLAB R2014a (MathWorks) was used to calculate the geometric means of PAC1 binding at different levels of integrin expression and to generate dot plots with the geometric means indicated as red dots, as previously described (Kim et al., 2009).

Cell imaging

CHO cells on gelatin-coated cover glasses were fixed with 3.7% formaldehyde and then permeabilized with phosphate-buffered saline (PBS) containing 0.1% Triton X-100 (PBS-t). After treatment with a blocking solution (10% goat serum and 0.5% gelatin in PBS-t), cells were stained with primary antibodies (anti-vimentin antibody and/or anti-HA antibody) and the appropriate fluorophore-conjugated secondary antibodies. After the cover glasses were mounted using Fluorescence Mounting Medium (Dako) containing Hoechst 33342 (Invitrogen), cells were observed under a fluorescence microscope (Ti-E, Nikon) equipped with a 100× (1.4 NA) plan-apochromat objective lens. More than ten microscopic fields were selected based on the expression of transfection marker, and the fluorescence images were collected by using a charge-coupled device camera (DS-Qi2, Nikon) and deconvoluted by using NIS-Elements AR (Nikon).

Cell migration assay

Upper chambers of a Transwell® culture plate with 8-µm pores (Corning) were incubated with 10 µg/ml fibrinogen in PBS overnight. A 4T1 cell suspension (5×10^4 cells/ml) was placed in the chamber, and cells were allowed to migrate through membrane pores during an incubation at 37°C in 5% CO_2 for 20 h. Next, cells were fixed and stained with Cell Staining Solution (Cell Biolabs). After washing with PBS, images of migrated cells on the opposite side of the membrane were captured with an inverted microscope (Motic AE2000). The number of migrated cells in each field was counted and the average number of triplicate samples was displayed as a bar graph with s.e.m.

In vivo metastasis assay

7-week-old female BALB/c mice were purchased from Orient Bio, Korea. Approximately 10^6 GFP-negative or -positive 4T1 cells in 100 µl PBS were injected into the tail veins of the mice (n=5 per each condition). After 2 weeks, all mice were killed with cervical dislocation and isolated lungs were frozen at −80°C before taking pictures with a digital camera. All the nodules displayed in the pictures were counted to generate the scatter plots. Animal studies were approved by the Institutional Animal Care and Use Committee of Korea University.

Acknowledgements

We thank Mark Ginsberg (University of California San Diego, CA) for his valuable input on this study.

Competing interests

The authors declare no competing or financial interests.

Author contributions

C.Y., J.K. and C.K. designed the research. M.G.K., H.J., D.P. and C.K. analyzed the data. C.Y., J.K., E.J.K., J.J., S.-J.K., S.M.K. and C.K. performed the experiments. C.Y., J.K. and C.K. wrote the paper, which was edited by M.G.K., H.J. and D.P.

Funding

This work was supported by the Basic Science Research Program through the National Research Foundation of Korea (NRF) and funded by the Ministry of Education [grant number NRF-2013R1A1A1007773]; and by a grant of the Korea Healthcare Technology R&D Project, Ministry of Health and Welfare, Republic of Korea [grant number HI14C0209].

Supplementary information

Supplementary information available online at
http://jcs.biologists.org/lookup/suppl/doi:10.1242/jcs.180315/-/DC1

References

Aslakson, C. J. and Miller, F. R. (1992). Selective events in the metastatic process defined by analysis of the sequential dissemination of subpopulations of a mouse mammary tumor. *Cancer Res.* **52**, 1399-1405.

Berrier, A. L., Mastrangelo, A. M., Downward, J., Ginsberg, M. and LaFlamme, S. E. (2000). Activated R-ras, Rac1, PI 3-kinase and PKCepsilon can each restore cell spreading inhibited by isolated integrin beta1 cytoplasmic domains. *J. Cell Biol.* **151**, 1549-1560.

Bhattacharya, R., Gonzalez, A. M., DeBiase, P. J., Trejo, H. E., Goldman, R. D., Flitney, F. W. and Jones, J. C. R. (2009). Recruitment of vimentin to the cell surface by beta3 integrin and plectin mediates adhesion strength. *J. Cell Sci.* **122**, 1390-1400.

Calderwood, D. A. (2004). Integrin activation. *J. Cell Sci.* **117**, 657-666.

Calderwood, D. A., Zent, R., Grant, R., Rees, D. J. G., Hynes, R. O. and Ginsberg, M. H. (1999). The Talin head domain binds to integrin beta subunit cytoplasmic tails and regulates integrin activation. *J. Biol. Chem.* **274**, 28071-28074.

Calderwood, D. A., Yan, B., de Pereda, J. M., Alvarez, B. G., Fujioka, Y., Liddington, R. C. and Ginsberg, M. H. (2002). The phosphotyrosine binding-like domain of talin activates integrins. *J. Biol. Chem.* **277**, 21749-21758.

Chang, Y.-C., Zhang, H., Franco-Barraza, J., Brennan, M. L., Patel, T., Cukierman, E. and Wu, J. (2014). Structural and mechanistic insights into the recruitment of talin by RIAM in integrin signaling. *Structure* **22**, 1810-1820.

Chernyatina, A. A., Nicolet, S., Aebi, U., Herrmann, H. and Strelkov, S. V. (2012). Atomic structure of the vimentin central alpha-helical domain and its implications for intermediate filament assembly. *Proc. Natl. Acad. Sci. USA* **109**, 13620-13625.

Correia, I., Chu, D., Chou, Y.-H., Goldman, R. D. and Matsudaira, P. (1999). Integrating the actin and vimentin cytoskeletons. *J. Cell Biol.* **146**, 831-842.

Eckes, B., Dogic, D., Colucci-Guyon, E., Wang, N., Maniotis, A., Ingber, D., Merckling, A., Langa, F., Aumailley, M., Delouvee, A. et al. (1998). Impaired mechanical stability, migration and contractile capacity in vimentin-deficient fibroblasts. *J. Cell Sci.* **111**, 1897-1907.

Eckes, B., Colucci-Guyon, E., Smola, H., Nodder, S., Babinet, C., Krieg, T. and Martin, P. (2000). Impaired wound healing in embryonic and adult mice lacking vimentin. *J. Cell Sci.* **113**, 2455-2462.

Elliott, P. R., Goult, B. T., Kopp, P. M., Bate, N., Grossmann, J. G., Roberts, G. C. K., Critchley, D. R. and Barsukov, I. L. (2010). The Structure of the talin head reveals a novel extended conformation of the FERM domain. *Structure* **18**, 1289-1299.

Gawecka, J. E., Griffiths, G. S., Ek-Rylander, B., Ramos, J. W. and Matter, M. L. (2010). R-Ras regulates migration through an interaction with filamin A in melanoma cells. *PLoS ONE* **5**, e11269.

Goldman, R. D., Khuon, S., Chou, Y. H., Opal, P. and Steinert, P. M. (1996). The function of intermediate filaments in cell shape and cytoskeletal integrity. *J. Cell Biol.* **134**, 971-983.

Gong, H., Shen, B., Flevaris, P., Chow, C., Lam, S. C.-T., Voyno-Yasenetskaya, T. A., Kozasa, T. and Du, X. (2010). G protein subunit Galpha13 binds to integrin alphaIIbbeta3 and mediates integrin "outside-in" signaling. *Science* **327**, 340-343.

Goodman, S. L. and Picard, M. (2012). Integrins as therapeutic targets. *Trends Pharmacol. Sci.* **33**, 405-412.

Gumbiner, B. M. (1996). Cell adhesion: the molecular basis of tissue architecture and morphogenesis. *Cell* **84**, 345-357.

Han, J., Lim, C. J., Watanabe, N., Soriani, A., Ratnikov, B., Calderwood, D. A., Puzon-McLaughlin, W., Lafuente, E. M., Boussiotis, V. A., Shattil, S. J. et al. (2006). Reconstructing and deconstructing agonist-induced activation of integrin alphaIIbbeta3. *Curr. Biol.* **16**, 1796-1806.

Harburger, D. S., Bouaouina, M. and Calderwood, D. A. (2009). Kindlin-1 and -2 directly bind the C-terminal region of beta integrin cytoplasmic tails and exert integrin-specific activation effects. *J. Biol. Chem.* **284**, 11485-11497.

Helfand, B. T., Mendez, M. G., Murthy, S. N. P., Shumaker, D. K., Grin, B., Mahammad, S., Aebi, U., Wedig, T., Wu, Y. I., Hahn, K. M. et al. (2011). Vimentin organization modulates the formation of lamellipodia. *Mol. Biol. Cell* **22**, 1274-1289.

Hughes, P. E., Renshaw, M. W., Pfaff, M., Forsyth, J., Keivens, V. M., Schwartz, M. A. and Ginsberg, M. H. (1997). Suppression of integrin activation: a novel function of a Ras/Raf-initiated MAP kinase pathway. *Cell* **88**, 521-530.

Hynes, R. O. (2002). Integrins: bidirectional, allosteric signaling machines. *Cell* **110**, 673-687.

Kim, C., Lau, T.-L., Ulmer, T. S. and Ginsberg, M. H. (2009). Interactions of platelet integrin alphaIIb and beta3 transmembrane domains in mammalian cell membranes and their role in integrin activation. *Blood* **113**, 4747-4753.

Kim, C., Ye, F. and Ginsberg, M. H. (2011). Regulation of integrin activation. *Annu. Rev. Cell Dev. Biol.* **27**, 321-345.

Kim, C., Schmidt, T., Cho, E.-G., Ye, F., Ulmer, T. S. and Ginsberg, M. H. (2012). Basic amino-acid side chains regulate transmembrane integrin signalling. *Nature* **481**, 209-213.

Kinbara, K., Goldfinger, L. E., Hansen, M., Chou, F.-L. and Ginsberg, M. H. (2003). Ras GTPases: integrins' friends or foes? *Nat. Rev. Mol. Cell Biol.* **4**, 767-778.

Lad, Y., Jiang, P., Ruskamo, S., Harburger, D. S., Ylanne, J., Campbell, I. D. and Calderwood, D. A. (2008). Structural basis of the migfilin-filamin interaction and competition with integrin beta tails. *J. Biol. Chem.* **283**, 35154-35163.

Langer-Gould, A., Atlas, S. W., Green, A. J., Bollen, A. W. and Pelletier, D. (2005). Progressive multifocal leukoencephalopathy in a patient treated with natalizumab. *N. Engl. J. Med.* **353**, 375-381.

Liu, Z., Zhang, B., Liu, K., Ding, Z. and Hu, X. (2012). Schisandrin B attenuates cancer invasion and metastasis via inhibiting epithelial-mesenchymal transition. *PLoS ONE* **7**, e40480.

Mendez, M. G., Kojima, S. and Goldman, R. D. (2010). Vimentin induces changes in cell shape, motility, and adhesion during the epithelial to mesenchymal transition. *FASEB J.* **24**, 1838-1851.

Moser, M., Legate, K. R., Zent, R. and Fassler, R. (2009). The tail of integrins, talin, and kindlins. *Science* **324**, 895-899.

Quinn, M. J., Byzova, T. V., Qin, J., Topol, E. J. and Plow, E. F. (2003). Integrin alphaIIbbeta3 and its antagonism. *Arterioscler. Thromb. Vasc. Biol.* **23**, 945-952.

Reynolds, A. R., Hart, I. R., Watson, A. R., Welti, J. C., Silva, R. G., Robinson, S. D., Da Violante, G., Gourlaouen, M., Salih, M., Jones, M. C. et al. (2009). Stimulation of tumor growth and angiogenesis by low concentrations of RGD-mimetic integrin inhibitors. *Nat. Med.* **15**, 392-400.

Satelli, A. and Li, S. (2011). Vimentin in cancer and its potential as a molecular target for cancer therapy. *Cell. Mol. Life Sci.* **68**, 3033-3046.

Shattil, S. J., Hoxie, J. A., Cunningham, M. and Brass, L. F. (1985). Changes in the platelet membrane glycoprotein IIb.IIIa complex during platelet activation. *J. Biol. Chem.* **260**, 11107-11114.

Shattil, S. J., Kim, C. and Ginsberg, M. H. (2010). The final steps of integrin activation: the end game. *Nat. Rev. Mol. Cell Biol.* **11**, 288-300.

Strelkov, S. V., Herrmann, H., Geisler, N., Wedig, T., Zimbelmann, R., Aebi, U. and Burkhard, P. (2002). Conserved segments 1A and 2B of the intermediate filament dimer: their atomic structures and role in filament assembly. *EMBO J.* **21**, 1255-1266.

Tadokoro, S., Shattil, S. J., Eto, K., Tai, V., Liddington, R. C., de Pereda, J. M., Ginsberg, M. H. and Calderwood, D. A. (2003). Talin binding to integrin beta tails: a final common step in integrin activation. *Science* **302**, 103-106.

Thiery, J. P. (2002). Epithelial–mesenchymal transitions in tumour progression. *Nat. Rev. Cancer* **2**, 442-454.

Tsuruta, D. and Jones, J. C. R. (2003). The vimentin cytoskeleton regulates focal contact size and adhesion of endothelial cells subjected to shear stress. *J. Cell Sci.* **116**, 4977-4984.

Wegener, K. L., Partridge, A. W., Han, J., Pickford, A. R., Liddington, R. C., Ginsberg, M. H. and Campbell, I. D. (2007). Structural basis of integrin activation by talin. *Cell* **128**, 171-182.

Wynne, J. P., Wu, J., Su, W., Mor, A., Patsoukis, N., Boussiotis, V. A., Hubbard, S. R. and Philips, M. R. (2012). Rap1-interacting adapter molecule (RIAM) associates with the plasma membrane via a proximity detector. *J. Cell Biol.* **199**, 317-339.

Yan, B., Calderwood, D. A., Yaspan, B. and Ginsberg, M. H. (2001). Calpain cleavage promotes talin binding to the beta 3 integrin cytoplasmic domain. *J. Biol. Chem.* **276**, 28164-28170.

Yang, J., Zhu, L., Zhang, H., Hirbawi, J., Fukuda, K., Dwivedi, P., Liu, J., Byzova, T., Plow, E. F., Wu, J. et al. (2014). Conformational activation of talin by RIAM triggers integrin-mediated cell adhesion. *Nat. Commun.* **5**, 5880.

Ye, F., Petrich, B. G., Anekal, P., Lefort, C. T., Kasirer-Friede, A., Shattil, S. J., Ruppert, R., Moser, M., Fässler, R. and Ginsberg, M. H. (2013). The mechanism of kindlin-mediated activation of integrin alphaIIbbeta3. *Curr. Biol.* **23**, 2288-2295.

Ye, F., Lagarrigue, F. and Ginsberg, M. H. (2014). SnapShot: talin and the modular nature of the integrin adhesome. *Cell* **156**, 1340-1340 e1.

Zhang, Z., Vuori, K., Wang, H.-G., Reed, J. C. and Ruoslahti, E. (1996). Integrin activation by R-ras. *Cell* **85**, 61-69.

Journal of Cell Science